Journal of Shellfish Research, Vol. 33, No. 1, 257–272, 2014.

THE EFFECTS OF AMBIENT AND AQUACULTURE STRUCTURE HYDRODYNAMICS ON THE FOOD SUPPLY AND DEMAND OF MUSSEL RAFTS

CARTER R. NEWELL[1]* AND JOHN RICHARDSON[2]

[1]*Maine Shellfish R+D, 7 Creek Lane, Damariscotta, ME 04543;* [2]*Blue Hill Hydraulics, 447 Falls Bridge Road, Blue Hill, ME 04614*

ABSTRACT A field and modeling study of the food supply and demand of mussel (*Mytilus edulis*) rafts in Maine established the hydrodynamic and particle consumption characteristics of shellfish aquaculture structures. Mussels on rafts filtered about 8×10^6 L/h and consumed about 40 g chlorophyll *a* (chl *a*)/h under favorable conditions. Because of the drag of the culture ropes and predator nets, velocity inside the rafts was reduced by 75%–80% in relation to ambient conditions. Chlorophyll consumption by mussels increased with increased food (chl *a*) concentration and also with increased water velocity inside the rafts. Clearance rates per raft also increased with food concentration. Model results allow for an estimation of water flux and seston depletion within the rafts through the use of point measurements and correction factors. Water velocity measurements taken mid depth in the middle of the rafts underestimated the mean flow through the raft by 10%. Measurements of current velocity and chl *a* concentration taken mid depth in the middle of the rafts underestimated the mean particle consumption rates by 13%. Model results and field data indicate that mussel raft hydrodynamics are a function of raft orientation to current direction, mussel raft size, raft aspect ratio, the presence of predator nets, the presence of multiple rafts, rope spacing, and rope diameter. Mussel raft design, placement, and biomass may be adjusted to optimize hydrodynamics and conditions favorable for improved mussel growth rates. Recommended flow speeds through experimental mussel rafts with a cross-sectional area of 121 m^2 require a minimum outside flow speed of 14–23 cm/sec.

KEY WORDS: hydrodynamics, mussel rafts, aquaculture

INTRODUCTION

Food consumption by mussels in floating rafts is a function of the flow through the rafts, mussel biomass and filtration rates, and ambient food concentrations. Characterization of the hydrodynamic properties of these suspended shellfish culture systems, and the effects of food concentration and ambient water velocity on mussel raft productivity have important implications for the aquaculture industry, in which alternate strategies of site selection, site management, and stocking densities may improve yields. It has been documented that mussel raft systems, which have a greater biomass of shellfish than longline systems, can remove a significant amount of phytoplankton, resulting in depletion within the rafts (Petersen et al. 2008), and impacting mussel growth and productivity (Fuentes et al. 2000). Several investigators have estimated the flow rates through mussel rafts, the depletion of food particles, and the effects of mussel raft biomass and density (Cabanas et al. 1979, Heasman et al. 1998, Camacho et al. 1991, Petersen et al. 2008). Duarte et al. (2008) demonstrated the importance of the drag of mussel ropes on mussel raft productivity, and the effects of mussel seeding density on the ropes have been studied (Cubillo et al. 2012), where there is also competition for space (Fréchette et al. 2010). Because there is competition for food within mussel rafts, it is useful to model the relationships between food supply and demand in these shellfish aquaculture structures.

The size, aspect ratio, and orientation (Delaux et al. 2011) of the suspended mussel culture systems, spacing of the culture ropes, individual rope diameter (Plew et al. 2009), shellfish biomass, and the presence of predator nets may affect water flow through the raft and therefore the supply of particles to the mussels. Previous field measurements of velocity distribution around mussel raft systems have been limited (Gibbs et al. 1991, Blanco et al. 1996, Boyd & Heasman 1998, Plew 2011a, Plew 2011b). Grant et al. (1998) suggested that raft-scale water exchange, which is a function of the drag coefficient of the mussel ropes (see also Duarte et al. (2008)), limits the secondary production of mussel rafts. Because drag is proportional to the square of the velocity, the current reduction within the raft resulting from drag should result in a mean velocity inside the raft being the square root of the ambient velocity. No previous workers have modeled in detail the effects of aquaculture structures (but see Delaux et al. (2011)) on ambient hydrodynamics and particle depletion using 3-dimensional computational fluid dynamics (CFD) techniques.

Although number of measurements may be made of flow velocity in the field, detailed 3-dimensional flow modeling can provide a more comprehensive understanding of the hydrodynamics of mussel rafts or raft systems, and can be used to predict the effects of different cultivation strategies to increase the productive capacity of the rafts. These strategies include site selection, orientation of the culture system, stocking densities, and the spatial distribution of biomass.

To determine the effects of ambient currents and husbandry practices on raft hydrodynamics and chlorophyll *a* (chl *a*; a tracer of total suspended particulate matter) consumption, flow simulations were performed using FLOW-3D, which is a CFD software package designed to analyze complex flows (Hirt 2010). Computational fluid dynamics involves the 3-dimensional solution of the governing equations for fluid flow (Navier–Stokes equations) at thousands of discrete points within the computational grid, and uses Reynold's number-dependent drag. FLOW-3D was used to understand detailed mussel raft hydrodynamics and the effects of various mussel raft parameters on the food supply and demand of these marine bivalve suspension culture systems. The raft hydrodynamics, which are a function of site-specific ambient conditions (e.g., tidal current velocities, directions, water depth, and wave climate) and mussel raft drag may also be characterized with respect to optimum flow conditions related to feeding (2–8 cm/sec (Newell

*Corresponding author. E-mail: musselsandoysters@gmail.com
DOI: 10.2983/035.033.0125

et al. 2001)) and sufficient particle flux such that depletion of chl *a* in the center of the raft is minimized.

The objectives of this study were to use a combination of field measurements and CFD models to investigate the hydrodynamic characteristics of mussel rafts in Maine, and to investigate the relationships between food concentration and water velocity on the clearance rates and food particle consumption rates of mussels in those rafts.

MATERIALS AND METHODS

Main Study Sites

Study sites were all located at commercial mussel raft cultivation sites in open coastal systems characterized by large tidal excursions and moderate maximum tidal velocities of 15–40 cm/sec. Mussel rafts were 12 × 12-m square rafts with 11-m-long mussel droppers, with an average of 400 lines per raft (2.8 droppers/m^2). Raft systems studied had either 2, 3, or 4 rafts moored in a row 5–10 m apart from each other. Study sites included Hardwood Island, Blue Hill Bay, and Northport, Belfast Bay (Fig. 1). Both sites had mean water depths of 20–25 m and a neap-to-spring tidal range of 3–4 m. Field measurements at the sites included vertical conductivity, temperature and depth (CTD) casts, current surveys along transects through the raft areas, feeding studies, measurements of mussel density and biomass, and longer term moorings of fluorometers and current meters. At all study sites, pegged mussel ropes or "droppers" were seeded in the fall (October) with seed mussels 0.5–3 cm long and harvested 12–16 mo later when the mussels grew to 5–7 cm long. In some cases, 2–3-cm-long mussels were also seeded on the culture ropes in the spring (May).

Experimental and Modeling Approach

A combination of field measurements and modeling was used in this study, and the approach is summarized in Table 1.

Site Hydrodynamics

Characterization of site hydrodynamics at control sites near the mussel rafts was performed by mooring an Interocean S4 electromagnetic current meter at mid depth and/or by using a bottom-mounted Sontek Acoustic Doppler Profiler (ADP) measuring in 2-m bins.

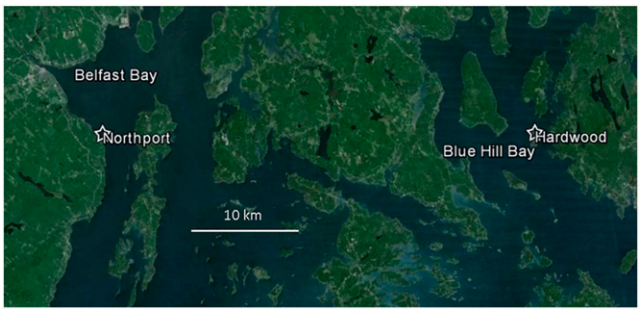

Figure 1. Location of main mussel raft lease sites studied in coastal Maine (from Google Earth). The Northport site is 44°22.155' N, 68°57.046' W and the Hardwood site is 44°18.435' N, 68°26.860' W.

TABLE 1.

Parameters affecting mussel raft productivity.

Site hydrodynamics	Measure	Moored instruments outside rafts
Raft hydrodynamics	Measure	Vertical profiles and transects
		Moored instruments inside rafts
		Effects of predator nets
	Model	Flow 3-dimensional velocity model
Food uptake	Measure	Vertical profiles and transects
		Moored instruments inside and outside rafts
		Water samples
		Mussel biomass and density
		Biodeposition studies
	Model	Flow 3-dimensional depletion model
Husbandry	Model	Raft length, number of rafts, orientation
		Number of ropes, rope diameter, biomass

Raft Hydrodynamics

Initially, the S4 was placed at 7 different locations within mussel rafts at Hardwood Island in 1999 to help tune the FLOW-3D raft model (described later). Also, the S4 was placed at mid depth (5.5 m from the surface) within fully seeded mussel rafts at Hardwood Island and Northport to determine flow speed and direction during several tidal cycles.

The Effects of Predator Nets

Water flow rates through mussel rafts with and without clean nets and with and without heavily fouled nets were measured to determine the range of flow reductions caused by nets on the mussel rafts. In January 2003, a Nortek acoustic Doppler velocimeter was placed in the middle of a seeded mussel raft at a 5-m depth for a period of 5 days. This raft had four clean 12-m-wide × 13-m-deep predator net panels composed of 3-mm polyethylene twine with a 10-cm square mesh that were sewn together on the sides and weighted on the bottom and corners. Water velocities were measured when the nets were in place for 2 days, after the nets were removed for 1 day, and again after they were rehung two more days. During a second period in 2012, the S4 electromagnetic current meter measured velocities at a 4-m depth from the surface in a mussel raft a at Clark's Cove, South Bristol, Maine (43°55.693' N, 69°34.384' W) with predator nets heavily fouled with tunicates. Measurements were made in the raft with predator nets for 3 days, and for 3 days after the end nets were removed.

Modeling Raft Velocity and Particle Consumption Using FLOW-3D

All the computations presented in this study were done using a fixed (Eulerian) grid of rectangular control volumes (Fig. 2) in a computational grid. Next the fractional area–volume–obstacle representation (FAVOR) method was used to define

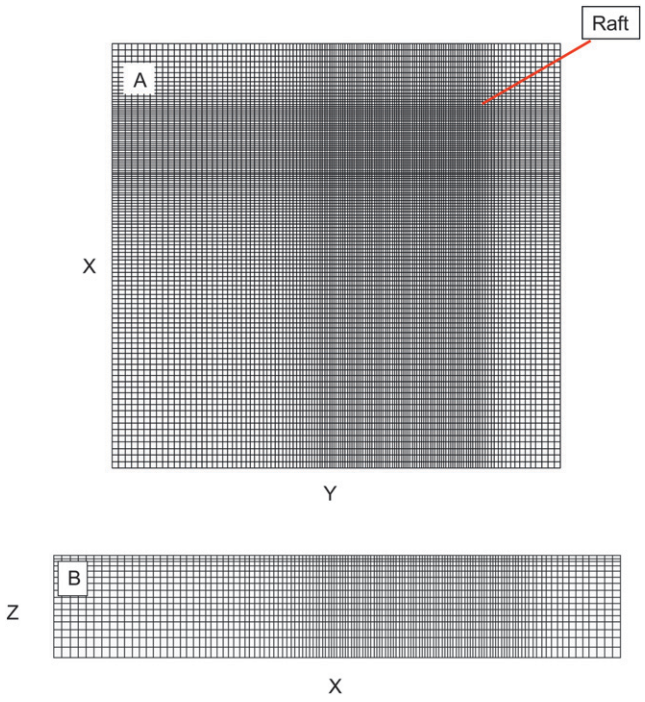

Figure 2. Structured grid used for CFD flow calculations. (A) The *x*–*y* plane (300 × 300 ft). (B) The *x*–*z* plane (300 × 60 ft).

general geometric regions within the rectangular grid. This method uses partial control volumes to provide the advantages of a body-fitted grid, but retains the construction simplicity of ordinary rectangular grids. The method also allows for the calculation of flow-through "porous" media (the regions beneath an aquaculture raft occupied by droppers). The FAVOR method was used to construct 2- and 3-dimensional models of a suspended rope aquaculture raft. Regions where droppers were present were assigned porosities according to the density of mussels found in those areas. Sections of mussel droppers were also measured with a meter stick using scuba to determine mussel rope diameters on seeded and mature grow-out lines. The ropes, when empty, were composed of either 1.25- or 1.6-cm-diameter polypropylene rope with a total of 35 polypropylene pegs, 22.9 cm long, placed every 31 cm along the rope to aid in mussel attachment. Size frequencies of the ropes yielded mean a rope diameters of approximately 10 cm for newly seeded lines, 20 cm for half-grown mussels, and 30 cm for market-size mussels (shell length, 5–7 cm), and these were used to develop drag coefficients and roughness parameters for the mussel rope elements in the model.

At the start of each CFD consumption simulation, phytoplankton concentrations were specified within the modeled region and at the upstream boundaries of the model. When underway, an advection–dispersion algorithm was used to calculate phytoplankton transport using a first-order upwind differencing scheme. To model phytoplankton consumption by mussels, the locations of cells occupied by mussels were stored in memory and, at the end of each time-step, the following logic was used to simulate feeding by the shellfish:

Computation involved looping through all control volumes in the computational grid as follows:

1. Check for the presence of mussels and phytoplankton in the current cell location.
2. If mussels and phytoplankton are present, then
   a. Adjust phytoplankton concentration in the current cell using the following equation:

$$P_n = P_c \times \left[1 - \left(\frac{N \times C_m \times dt}{dx \times dy \times dz}\right)\right], \quad (1)$$

   where P_n is the new phytoplankton concentration, P_c is the current phytoplankton concentration, N is the number of mussels, C_m is the clearance rate of 1 mussel, and dx, dy, and dz are cell size; and units are concentration equal to mass divided by length cubed, dt equal to the change in time, C_m equal to length cubed divided by time, and dx, dy, and dz are computational cell size measured as length cubed. If P_n is less than 0.0, then reset to 0.0
   b. Go to 4.
3. If mussels and phytoplankton are not present, then go to 4.
4. Move to next cell location and return to 1.
5. End after all cells in the computational grid have been checked and proceed with the next simulation time-step.

Individual mussel filtration rates were determined from *in situ* biodeposition studies (discussed later). The results of these CFD consumption calculations provide estimates of phytoplankton concentrations throughout the rafts. In this way, mussel rope size and density of the rafts can be evaluated relative to local hydrodynamic conditions and food availability. Although simple, the resulting algorithm works well within the structure of the FLOW-3D program, which is based on an explicit solution scheme in which the size of the time-step is limited. With appropriate-size time-steps, the amount of consumption per cycle is small and the algorithm produces numerical, stable, and accurate solutions.

The results of the consumption calculations provided estimates of phytoplankton concentrations throughout the rafts, reflecting the variations in water velocities and the distribution of biomass supplied to the model. In this way, mussel dropper size and density on the rafts could be evaluated relative to food availability and hydrodynamic conditions as they varied throughout the raft.

Once the mussel raft CFD model was calibrated, the actual volume flux (VF) and chl *a* consumption integrated throughout the entire raft could be estimated using the numerical solution, where $VF_{\text{actual}} = VF_{\text{measured}} \times F$ (a conversion factor). Then, the water VF and food consumption of the whole raft were estimated from field measurements of velocity and chl *a* at 1 location only (in the middle of a mussel raft at mid depth).

Modeling Raft Velocity Using FLOW-3D

The flow in the model domain was controlled by boundary conditions obtained from field data and set upstream (fluid velocity and depth), downstream (depth), and at the fluid-free surface (atmospheric pressure and 0 shear). In addition, a no-slip condition was specified at solid boundaries within the model domain, which included raft structures (floats and droppers) within the computational grid. These same boundary conditions were used for all the calculations made. The flow calculations began approximately 1.5 raft lengths upstream of the subject structure. The mean upstream flow velocity = 0.168 m/sec was derived from the mean flow velocity at Hardwood

Island North in June 1999. The floats of the mussel rafts were modeled as solid obstacles in FLOW-3D whereas the arrays of ropes hanging from the raft were modeled as porous obstacles (as described earlier). The model setup is presented in Table 2.

Sampling Locations for Measuring Mussel Raft Flow Rates and Particle Consumption Rates: Model Calibration

To examine how flow measurement at one location in the raft (in the center at a mid depth of 5.5 m) could be used to estimate the mean flow speed throughout the entire raft, steady flow patterns were calculated using the calibrated FLOW-3D model. Six sample locations were chosen within the raft to determine which location gave the closest estimate of mean velocity in the entire raft (or smallest error).

Effects of Raft Culture Systems on Flow Through Rafts

Once the FLOW-3D hydrodynamic model was calibrated for the rafts, a number of hypothetical scenarios were examined concerning the size, aspect ratio, orientation, dropper diameter, and rope spacing on the mean water velocity inside the rafts. Field data from Hardwood Island (mean velocity, 16.8 cm/sec; orientation of flow direction, 45 deg) was used as initial conditions for the FLOW-3D simulations. These modeling results were used to develop a series of recommendations concerning the optimization of mussel raft systems in tidal waters by increasing water flow through the rafts.

Determination of Clearance Rates and Food Particle Consumption Rates by Mussels in a Raft

Total clearance rates of mussels in a raft were determined using the method of Coughlan (1969), which accounts for the progressive dilution of food particles as they pass through a mussel raft. Applying Coughlan's equation to a mussel raft results in the total clearance by mussels in a raft (Cr):

$$C_r = \left(\frac{M}{n \times t}\right) \times \ln\left(\frac{C_o}{C_t}\right), \tag{2}$$

where M is the volume of suspension (equal to mussel raft volume, length × width × depth), t is time (time for water to pass through the raft), n is the number of mussels in the raft, C_o is the initial concentration (equal to the concentration upstream of raft), and C_t is the concentration at time t (equal to the concentration at the end of the raft).

Multiplying both sides by n and substituting VF flux within raft for M/T, we get a clearance rate of the raft:

$$C_r = VF \times \ln\left(\frac{C_o}{C_t}\right). \tag{3}$$

In the current study, the VF was calculated as the mean current speed within the raft (U) multiplied by the raft cross-sectional area normal to flow direction (i.e., 12-m-wide rafts × 11-m-deep droppers). For square or rectangular mussel rafts with fixed mooring systems, the raft cross-sectional area may also vary with its orientation relative to ambient flow direction. If the settling rate (s) of chl *a* in a control volume is measured (Coughlan 1969), the formula would be

$$C_r = \text{Flow rate} \times \left[\ln\left(\frac{C_o}{C_t}\right) - s\right]. \tag{4}$$

Chlorophyll *a* consumption rate (C_{chla}) by mussels in a raft (equal to chl *a* filtration rate) were calculated in the in the following manner (Bayne et al. 1993), assuming a steady state:

$$C_{chla} = \text{Flow rate} \times (C_o - C_t). \tag{5}$$

Consumption rates of carbon, nitrogen, phytoplankton, and particulate organic matter were determined in a similar way.

Vertical Profiles and Transects

Two mussel rafts at Hardwood Island, Blue Hill Bay, were used to measure vertical profiles of current speed and phytoplankton fluorescence along transects upstream, in the front, middle, and downstream locations of the rafts (Fig. 3) in September 1999. This characterized the effects of rafts on ambient hydrodynamics and seston levels at 4 tidal stages: flood (or incoming) tide, high tide, ebb (or outgoing) tide, and low tide. An Interocean S4 current meter and a Seabird 19-Plus CTD with a Wet Star fluorescence probe were used for the profiles at 0.5-sec sampling intervals for 1 min at 7 vertical locations at 3-m depth intervals 4–22 m from the surface.

Clearance and Chlorophyll a *Consumption Rates of Mussels in a Raft*

Profiles of current speed and chl *a* were made using the S4 current meter and a Seabird 19-plus during September 20 and 21, 1999, at Hardwood Island during 4 tidal stages, and on November 24, 2002, at 1 tidal stage. In June 2002, chl *a* profiles

TABLE 2.

Model setup (3-dimensional calculation).

Control volume (m)	.902 × 0.092 × 0.902
Total no. of control volumes	300,000
Flow	Steady
Boundary conditions	Velocity
Angle of incidence (deg)	45
Average flow speed (m/sec)	0.168
Typical rope diameter (m)	0.3

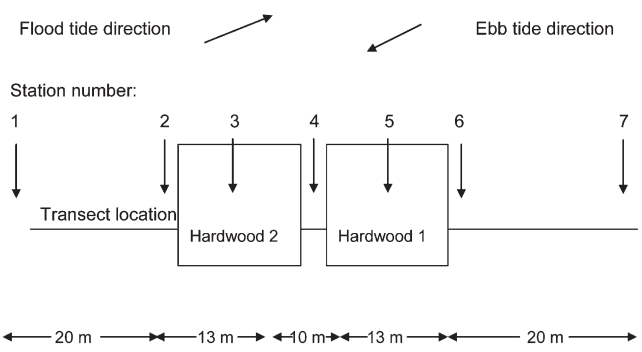

Figure 3. Sample locations for profiles of current speed and fluorescence at Hardwood Island, Maine, in September 1999. Total water depth was 25 m; profiles were at 3-m intervals from 4–22 m in depth.

were made but current speed was obtained from mid depth only in the middle of the raft. In 2001 and 2002, vertical profiles of fluorescence were made along transect locations through 3 and 4 raft arrays at Hardwood Island and Northport, Maine, and were bin averaged at 2-m depth intervals whereas the S4 measured flow through the rafts. The profile data were used to determine values of the depth integrated U, C_o, and C_t for determination of Cr and C_{chla}. Longer term measurements of clearance and chl *a* consumption rates were accomplished using the S4 and Seabird at mid depth outside and inside the mussel rafts. During two periods in January and one during June 2002 at Hardwood Island, and during July 2002 at Northport, chl *a* consumption was also estimated over 2–4 day periods using two YSI Sondes at a 5-m depth. One was stationed inside the center of the raft next to the S4 current meter at a 5-m depth and the other (control) probe was placed outside the raft.

It is important to determine whether either outside food concentration (C_o) or water velocity (U) is associated with changes in the clearance rate (C_r) or food consumption rate (C_{chla}) of mussels feeding in the rafts to predict the effects of different management strategies on mussel raft productivity. Because both the clearance rates and chl *a* consumption rates (Eq (3) and Eq (5)) have outside chl *a* concentration and water velocity in their formulations, they are not independent. The correlations among environmental variables U and $C_{o,}$ and C_r and C_{chla} were examined using the Pearson product moment correlation coefficient, and then a least squares linear regression analysis was used to model the effects of either environmental variable on mussel filtration rates or chl *a* consumption rates with the linear model:

$$C_r \text{ or } C_{chla} = \text{Constant} + b(x). \tag{6}$$

Water Samples

In addition to using water velocity and phytoplankton fluorescence profiles to characterize mussel raft effects on flow and seston, a DC-powered pump and manifold system was used to pump water samples from the mussel raft at mid depth (depth, 5 m) at 5 horizontal locations, and 1 location under the raft (station 6) 3 m below the mussel ropes in the middle of the raft (Fig. 4). Samples were pumped to a central manifold at times based on current meter measurements such that a single parcel of water was followed through the mussel raft. One- to 2-L samples were prefiltered with a 243-μm mesh to remove zooplankton, and were filtered on prewashed and preashed GFC filters to determine the dry mass of suspended particulate matter (SPM), particulate organic matter, and particulate inorganic matter (PIM) after rinsing with isotonic ammonium formate. Suspended particulate matter was determined after drying for 24 h at 85°C, and ash weight was determined after samples were ignited in a muffle furnace for 3 h at 450°C. Subsamples of 0.25 L were taken for particulate organic carbon and nitrogen (POC and PON, respectively) and chlorophyll analysis. The POC and PON samples were frozen until analyzed, dried and fumed with HCl to remove carbonates, and analyzed for POC and PON on a Perkins-Elmer analyzer. Chlorophyll *a* was determined from freshly collected seawater samples (250 mL) that were filtered through 25 mm Whatman GFC glass fiber filters using gentle vacuum, and were then frozen. After extraction, samples were brought to room temperature in the dark, and fluorescence before and after acidification with 1 N HCl was measured using a Turner Designs model 10–005R fluorometer. Data were reported according to Yentsch and Menzel (1963).

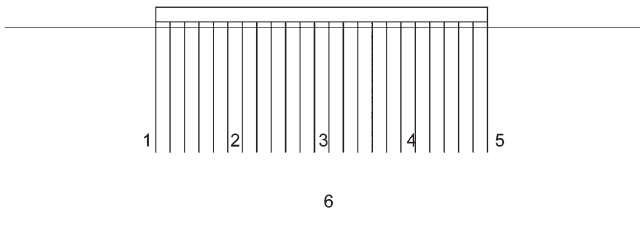

Figure 4. Sample locations for pumped water samples taken from Hardwood 2 in September 1999.

Subsamples were also fixed in Lugol's iodine for the determination of phytoplankton biomass (2-mL settled samples that converted into carbon using the method of Strathmann (1967)). Water samples for extracted chl *a* were taken periodically with CTD casts to calibrate the *in vivo* fluorescence with extracted chl *a*.

Water samples were also taken upstream of the mussel rafts in spring, summer, and fall 2002 at Hardwood Island and Northport for POC and chl *a* to estimate POC uptake from the rafts from the CTD data.

Mussel Raft Biomass and Density

For biomass and density determinations, mussel samples were taken from standard distances along mussel droppers at different depths and analyzed for shell length, weight, count, and volume (number of mussels per liter), and for subsamples of 30–40 mussels over the size range observed to determine the dry tissue weight (24 h at 80°C) as well as the shell length (Newell 1990). The mean shell length of the bulk sample was determined using the shell length to count per-liter regression developed for Maine blue mussels (Newell 1990):

$$\text{Shell length (mm)} = \frac{10^{7.97 - log_{10}(\text{No. mussels}/35.2\,\text{L})}}{2.74}. \tag{7}$$

The dry tissue weight for the corresponding mean shell length was then estimated from the least squares regression coefficients of the log_{10} shell length to log_{10} dry tissue weight plots.

To estimate total mussel raft biomass, a crane scale was used to measure dropper weights throughout the raft in the water, and then in the air, and samples from different sites and times of year yielded a general relationship:

$$\frac{\text{Weight of droppers in the water}}{\text{Weight of mussels in air}} = 0.25. \tag{8}$$

A regression between mussel dry tissue weight (M_d) and mussel total (including shell) live weight (M_t) was established for market-size mussels at Hardwood Island on January 22, 2002 ($n = 30$, $r^2 = 0.78$):

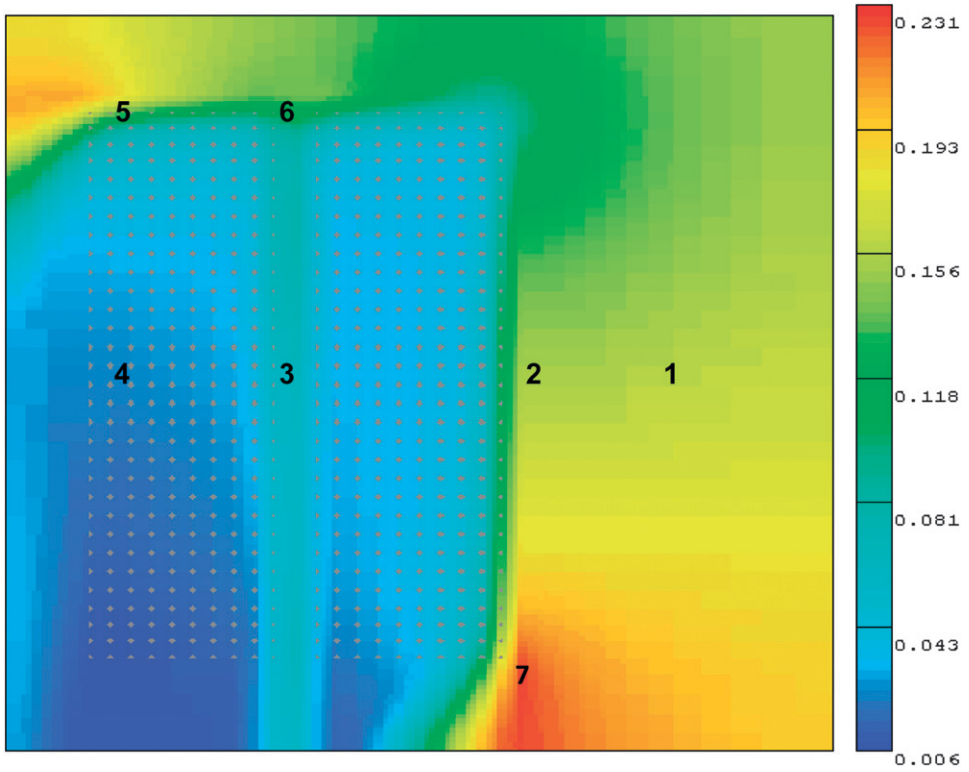

Figure 5. Locations of velocity measurements, and modeled velocity (colored by magnitude measured in meters per second) at a depth of 5.5 m below the surface (see Table 2).

$$M_d = (M_t \times 0.108) - 0.507. \quad (9)$$

The dry tissue biomass of the entire mussel raft was then estimated multiplying M_d by the number of mussels on the raft.

Biodeposition Studies

Using flow-through chambers and the biodeposition method, we were able to estimate particle consumption by individual mussels (in contrast to the total raft) in the field at Hardwood Island on September 9, 2000. Water was pumped from 1 m below the surface using a DC centrifugal pump into a head tank, and was then gravity fed to three chambers housing mussels and one empty control chamber for 10 h. It was sampled hourly for the PIM content of the available seston. Flow rates were maintained at approximately 200 mL/min (equal to 12 L/h). The PIM content of the biodeposits from the mussel chambers was used to determine the volume filtered using the ash tracer method (Iglesias et al. 1992). The biodeposits were collected and analyzed for the weight of PIM in the feces. Because the inorganic matter is not assimilated by the mussels and its concentration in the SPM can be characterized, the amount of inorganic matter in the feces can be considered an indicator of volume filtered by the mussels. Samples were corrected for sedimentation in control chambers without mussels. Individual mussel clearance rate (measured in liters per hour) was calculated as

$$C_r = \frac{\text{PIM egestion rate (milligrams per hour)}}{\text{PIM (milligrams per liter)}}. \quad (10)$$

RESULTS

Mussel Raft Hydrodynamics

Current velocity and direction over a tidal cycle inside mussel rafts measured at a 5.5-m depth from the surface in the middle of the rafts ranged from 0–4 cm/sec (Hardwood Island) to 0–8 cm/sec (Northport). Mean current speed in the Northport raft (4.3 cm/sec) was about twice as high as the Hardwood Island raft (1.7 cm/sec). Although flood and ebb directions were generally north and south in both locations, flow directions varied considerably over each tidal stage.

TABLE 3.

Velocity magnitude (measured in centimeter per seconds) at a depth of 5 m.

Location	1	2	3	4	5	6	7
Measured data	13.6	9	6	3.1	12.2	9.7	4.7
Calculated data	17	13	7	3	17	11	6

See Figure 5.

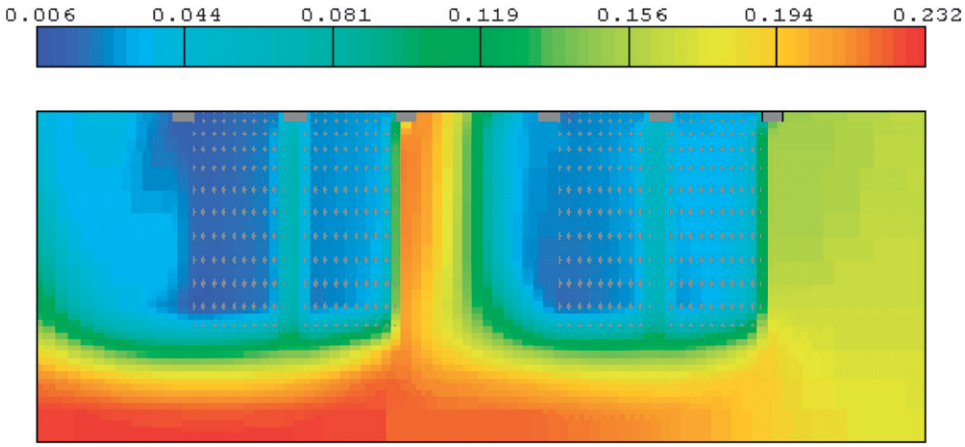

Figure 6. Profile view of velocity magnitude (measured in meters per second) around 2 mussel rafts with an approach angle of 45 deg.

Site Hydrodynamics

Flow measured using the ADP outside the mussel rafts in Northport, and measured inside the middle of a raft at a depth of 5 m with a Nortek ADV over the same tidal cycle on January 29, 2003, demonstrated significant attenuation within the raft. Mean current speed (±SE) inside the raft was 3.51 ± 0.18 cm/sec, and outside the raft was 15.1 ± 0.98 cm/sec. Thus, flow speed inside the raft was about 23% of the flow outside the raft. Modeled flow attenuation inside the raft was found to be 21.4% of the ambient velocity using FLOW-3D (discussed later). Flow direction inside and outside the raft were similar during the same time period. The ADP also recorded flow over 17.5 tidal cycles in Northport during a windy period in January 2003. Mean velocity recorded throughout the entire water column was 17.5 cm/sec (maximum, 30 cm/sec), whereas the mean velocity recorded at the upper 2 m of the water column was 30.0 cm/sec (maximum, 83.3 cm/sec) resulting from wind-driven circulation.

Effects of Predator Nets

The mean velocity at the 5-m depth (measured every 10 min over 5 days) at Northport in 2003, when predator nets were in place, removed, and replaced, resulted in a 25.4% reduction in mean flow speed inside the raft as a result of the predator nets, which were not fouled with algae. In comparison, in 2012, the mean water velocity inside the mussel rafts at Clark's Cove, with heavily fouled predator nets (0.81 ± 0.03 (SE) cm/sec) was 5 times slower than when the nets were removed (4.04 ± 0.05 cm/sec).

Modeling Raft Velocity and Particle Depletion Using FLOW-3D

The velocities calculated using the numerical model were compared with the velocity measurements taken around the mussel rafts (Fig. 5, Table 3) during model calibration. The CFD flow model provides a spatially complete and descriptive picture of the flow through the raft system (Figs. 5, 6, and 7). From 9 locations within the raft (Fig. 8), the actual mean water velocity over the entire raft was underestimated by 10% by a convenient point measurement in the middle at mid depth (Table 4). This 10% correction factor was then used in the determination of mussel raft VF in subsequent estimations of mussel raft filtration rate and consumption rate:

$$VF_{\text{actual}} = VF_{\text{measured}} \times 1.1. \quad (11)$$

The CFD model was also used to examine how sampling chl *a* at 1 location (location 1, Fig. 7) could provide a good estimate of the total consumption of chl *a* by mussels in a raft. In this case, the errors indicate how the sample locations of point measurements affect the estimation of mean mussel raft chl *a* consumption. Measurements in the middle of the raft at a 5.5-m depth underestimate total particle consumption by 13% (Table 5), such that

$$\text{Consumption}_{\text{actual}} = \text{Consumption}_{\text{measured}} \times 1.13. \quad (12)$$

The CFD depletion model provides a spatially complete and descriptive picture of food availability within the mussel raft (Fig. 9).

Vertical Profiles and Transects

Current speed and *in vivo* fluorescence profiles through the mussel raft system on September 20, 1999, with respect to sample station, are presented in Figure 10. Water accelerated under the raft and below 11 m, where the ropes hang. Slightly greater velocities were observed near the sea surface. It was also noted that about 50% of the chl *a* was depleted within the rafts at stations 3 and 5 on the flood tide. Using fluorescence values from depths within the mussel rafts (at 4, 7, and 10 m), the effects of tidal stage on food availability within the 2 raft systems were also investigated. Periods of greater fluorescence alternate between flood and ebb tides, and at low tide there are generally low food levels throughout the mussel raft array.

Water Samples

Seston carbon and nitrogen from pumped water samples (Fig. 4) at Hardwood Island in September 1999 showed a similar result to the fluorescence, where concentrations were reduced by about 50% in the downstream direction within the rafts (Fig. 11). Note that at station 6, which is suspended below the raft, POC levels are greater than within the raft. This may the

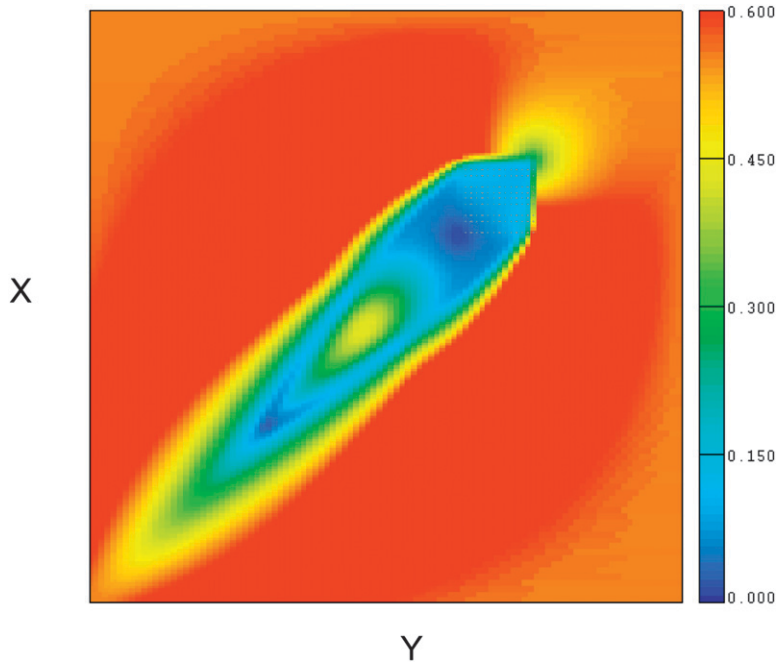

Figure 7. Flow through the raft (colored by speed; measured in centimeters per second) at a depth of 5.5 m from the surface.

result of flow under the raft in addition to the settling of mussel biodeposits. Phytoplankton carbon at slack tide on September 9 and on the flood tide on September 1 gave similar results to the fluorescence and POC and PON analyses presented earlier. To estimate the uptake of POC from the rafts, we sampled POC (measured in milligrams per liter) and chl *a* (measured in micrograms per liter) in the spring, summer, and fall in 2002. The regression equations relating POC to chl *a* were as follows:

$$\text{For Hardwood Island}\left(n = 9,\ R^2 = 0.702\right):$$
$$\text{POC} = 12.79 \times (\text{chl}\,a) + 29.9. \quad (13)$$

$$\text{For Northport}\left(n = 10,\ R^2 = 0.814\right)$$
$$\text{POC} = 12.58 \times (\text{chl}\,a) + 54.3. \quad (14)$$

These equations were used to estimate POC uptake from the rafts to compare with other studies on mussel rafts.

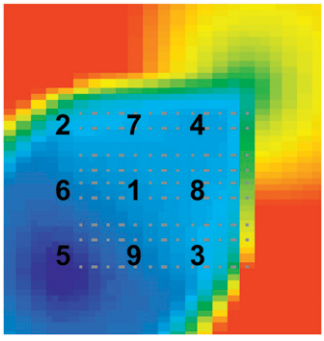

Figure 8. Velocity measurement locations in mussel raft for determination of mussel raft volume flux (see Table 3).

Mussel Clearance and Chlorophyll *a* Consumption Rates

The profiles were used to calculate mussel raft clearance rates and chl *a* consumption rates as described in the Methods section. Mean clearance rates ranged from $2–14 \times 10^6$ L/h and chl *a* consumption rates varied from 9–84 g chl *a*/h. Values in September 1999 for Hardwood 1 and Hardwood 2 rafts are means from profiles taken on flood, ebb, high, and low tides, and are more representative of daily average rates. Data from only 1 tidal stage (June and November) are more extreme than the daily average rates.

In contrast to the profiles, continuous measurements from current meters and CTD moorings provide a better of the effects of different environmental conditions on particle clearance and food consumption by mussels in the rafts. Mean daily clearance rates ranged from $1–5 \times 10^6$ L/h and chl *a* consumption rates varied from 5–25 g chl *a*/h (Fig. 12). Correlation analysis using the Pearson product moment correlation coefficient, established that U and C_o correlated significantly with mussel raft consumption and, in most cases, also with mussel raft clearance rate. The effects of current speed and chl *a* concentration

TABLE 4.

Flux calculation summary.

Measurements	V_{avg} (cm/sec)	Flux (m^3/sec)	Error (%)
Actual	3.3	1.78	N/A
Point no. 1	3.1	1.61	–10
Point nos. 1, 2, and 3	4.8	2.64	+48
Point nos. 1, 2, 3, 4, and 5	4.0	2.09	+17
Point nos. 6, 7, 8, and 9	3.1	1.59	–11
Point nos. 1, 6, 7, 8, and 9	3.1	1.59	–11

TABLE 5.

Consumption calculation summary.

Measurements	V_{avg} (cm/sec)	Flux (m^3/sec)	Error (%)	Concentration (μg/L)	Error (%)	Consumption (μg/sec)	Error (%)
Force window*	3.3	1.78	N/A	3.12	N/A	3,985	N/A
Point no. 1	3.1	1.61	–10	3.85	+23	3,460	–13
Point nos. 1, 2, and 3	4.8	2.64	+48	4.9	+58	2,905	–29
Point nos. 1, 2, 3, 4, and 5	4.0	2.09	+17	4.4	+40	3,341	–14
Point nos. 6, 7, 8, and 9	3.1	1.59	–11	4.1	+30	3,009	–23
Point nos. 1, 6, 7, 8, and 9	3.1	1.59	–11	4.0	+29	3,179	–21

* Force window is the mean value through the entire mussel raft based on CFD modeling. Other measurement locations (Fig. 7) illustrate how the location of water velocity or chl *a* concentration measurements relate to mean raft values.

outside of the rafts on clearance rate and chl *a* consumption rate are summarized in Table 6. In all cases, the chl *a* concentration outside the raft had a significant positive effect on mussel raft daily consumption rate. Current speed had a significant positive effect on clearance rate during 3 of the 4 periods studied. During the lowest food period (June 12–13, 2002), both current speed and outside chl *a* had a significant, positive effect on mussel clearance rate and chl *a* consumption rate.

Because the control CTD outside the rafts during the long-term studies of mussel rafts was sometimes downstream of the mussel rafts over long-term (daily) periods, the data were reanalyzed using current directions only when the control CTD was upstream (Fig. 13). During these periods (2.5–10 h), with sampling periods of 1–10 min, food consumption and particle clearance rates were always correlated significantly and positively with outside chl *a*, and food consumption was always correlated significantly and positively with current speed (Table 7). During two of the 4 periods, clearance rate also correlated significantly and positively with current speed. Particle clearance rates by mussels in the rafts had maximum values of 2×10^7 L/h during each of the 4 periods studied, and maximum chl *a* consumption rates were 80–100 g/h. Mean consumption rates for each period were lower at Hardwood Island (25–33 g/h) than at Northport (52 g/h), as were clearance rates ($7–9 \times 10^6$ L/h at Hardwood vs. 14.5×10^6 at Northport).

Consumption rates of POC may be estimated from the regressions of POC to chl *a* for each of the sites. Using mean chl *a* consumption data from Figure 13 and the previous POC/chl *a* regressions, the mean daily POC consumption by mussels in the rafts at Hardwood Island and Northport were estimated. Consumption rates of POC at Hardwood on January 10, January 23, and June 12, 2002, was 418 g/h/raft, 390 g/h/raft, and 116 g/h/raft, respectively, and at Northport in July 2002, POC consumption was 326 g/h/raft.

Mussel Raft Biomass and Density

Mussel density and biomass were determined at 10 mo and 14 mo after seeding in 1999 at Hardwood Island, and 8–16 mo after seeding at Hardwood Island and Northport in 2002 and 2003 (Table 8). Mussel raft biomass was used to provide an input for the CFD consumption modeling (described earlier).

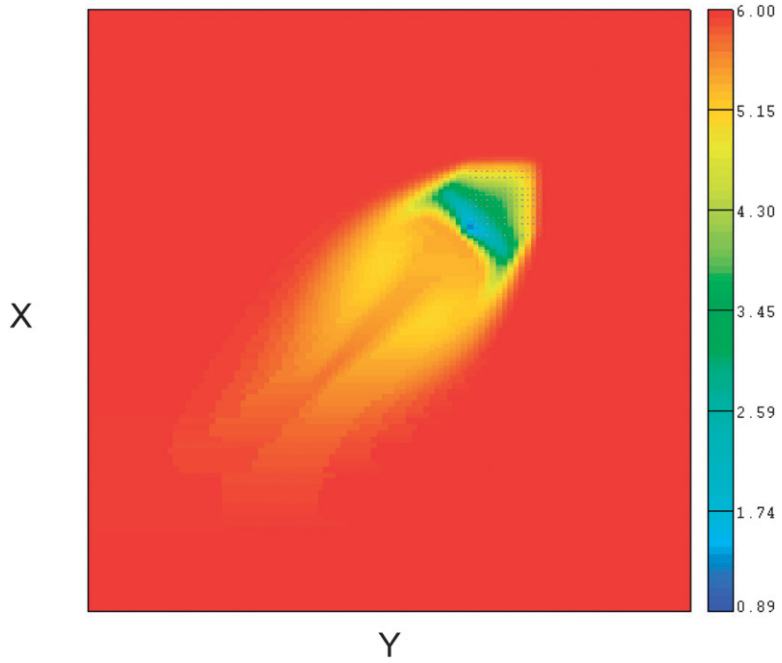

Figure 9. Chlorophyll *a* concentration in raft (colored by concentration; measured in micrograms per liter) at a depth of 5.5 m from the surface.

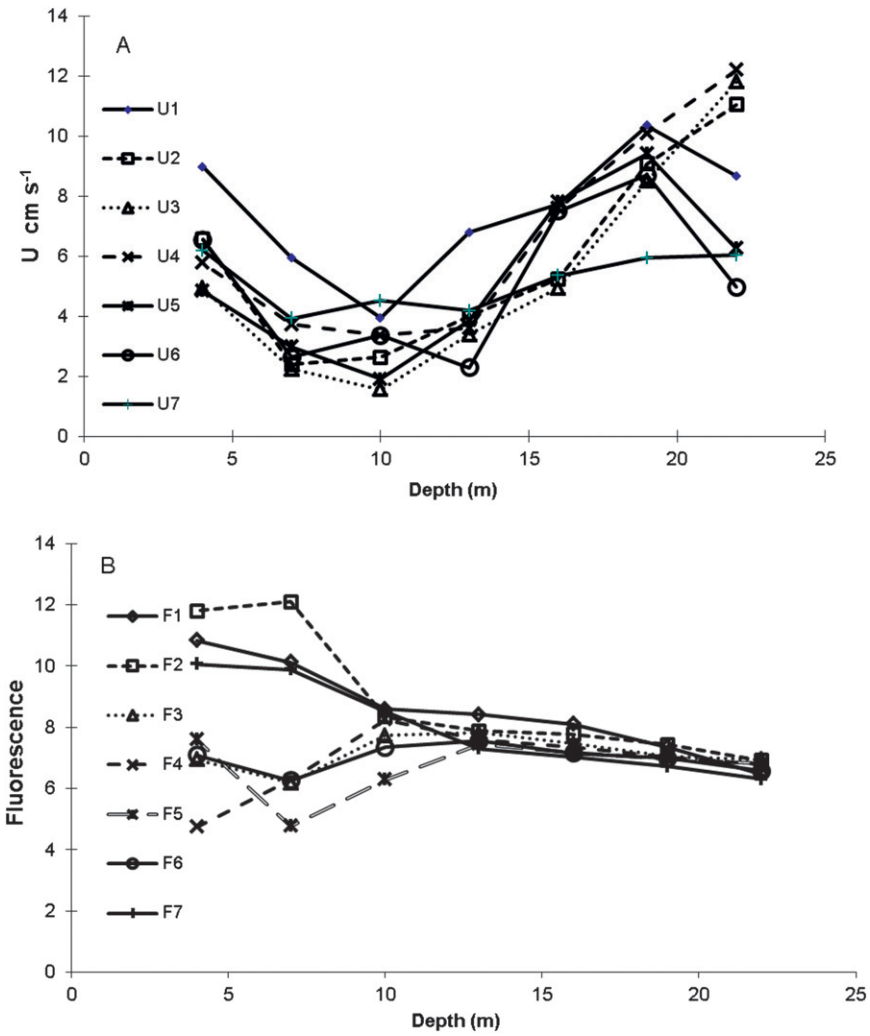

Figure 10. (A, B) Flood tide water velocity (A) and fluorescence (B) with respect to water depth (measured in meters) at Hardwood Island mussel rafts on September 20, 1999. For sample locations, see Figure 3.

Throughout the entire sampling period, mean (±SE) mussel density, rope dry tissue biomass, and raft dry tissue biomass were 914 ± 92 mussels/m, 0.896 ± 85 kg/m, and 3,941 ± 369 kg/raft, respectively. Biomass reached an asymptotic level of about 1,300 g/m at a density of about 1,300 mussel/m. Mussel biomass (b) was related to density (d) by the Eq (15) ($r^2 = 0.46$, $n = 29$, $P = 0.0001$):

$$b = 0.004\left(d^2\right) + 1.42(d) + 42.9. \quad (15)$$

Mussel raft biomass was also estimated using Eq (9) during harvest operations. Samples of 60 mussels from 29 mussel harvests between January 2002 and April 2002 were analyzed for mussel live weight and mean shell length. Mean dry tissue weight and shell length (±SE) determined using Eq (9) was 1.8 ± 0.06 g and 6.36 ± 0.97 cm, respectively. Using mean density above (914/m) and 400 × 11-m culture ropes on each raft, the total raft dry tissue weight biomass of market-sized mussels at harvest was estimated to be 7,240 kg/raft.

Biodeposition Studies

On September 8, 1999, 3 mussels in individual feeding chambers for 10.5 h had a mean (±SE) clearance rate of 4.3 ± 0.54 L/h with a PIM content of the seston of 0.54 ± 0.05 mg/L. These clearance rates (for a given biomass) were used in the CFD consumption models (described earlier).

Model Results of the Effects of Raft Culture Systems on Flow Through Rafts

The following equations, calculated using the results of CFD model runs, predict the mean water velocity (V) through mussel rafts, using the Hardwood Island conditions presented in Table 2.

$$\text{Raft length } (L)\text{: } V(\text{centimeters/second}) = 0.0837\ \text{L}^{-0.3963} \quad (16)$$

$$\text{Number of rafts } (N) 10\text{ m apart: } V = 0.655\,N + 2.05 \quad (17)$$

$$\text{Orientation (square raft), front: } V = 2.55,\ 45\text{ deg: } V = 4.95$$

$$\text{Aspect ration } (R, \text{ length divided by width}): V = 4.45\ R^{-0.19} (\text{Fig. 14}) \quad (18)$$

Number of ropes and rope diameter (x, measured in centimeters:

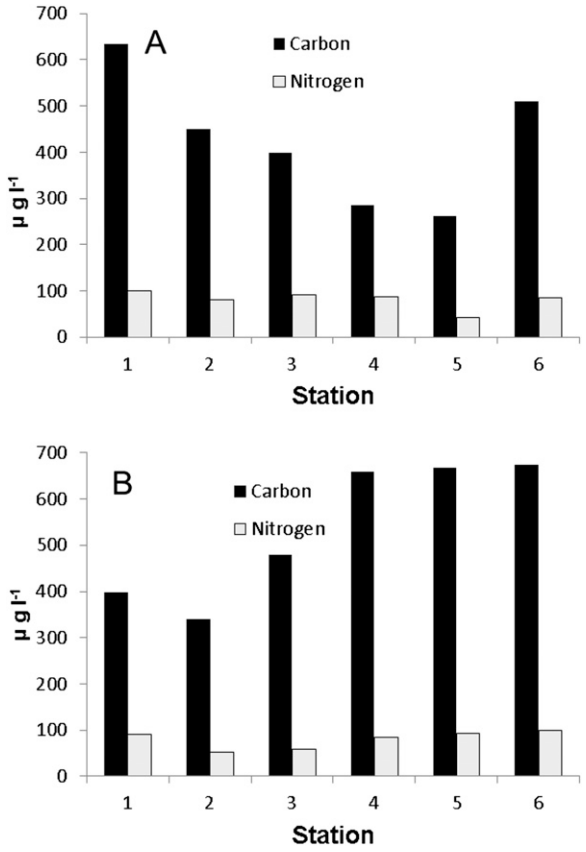

Figure 11. (A, B) Particulate carbon and nitrogen at a 5-m depth from pumped samples at the Hardwood 2 raft in September 1999 on flood (A) and ebb (B) tides. Station locations are presented in Figure 4.

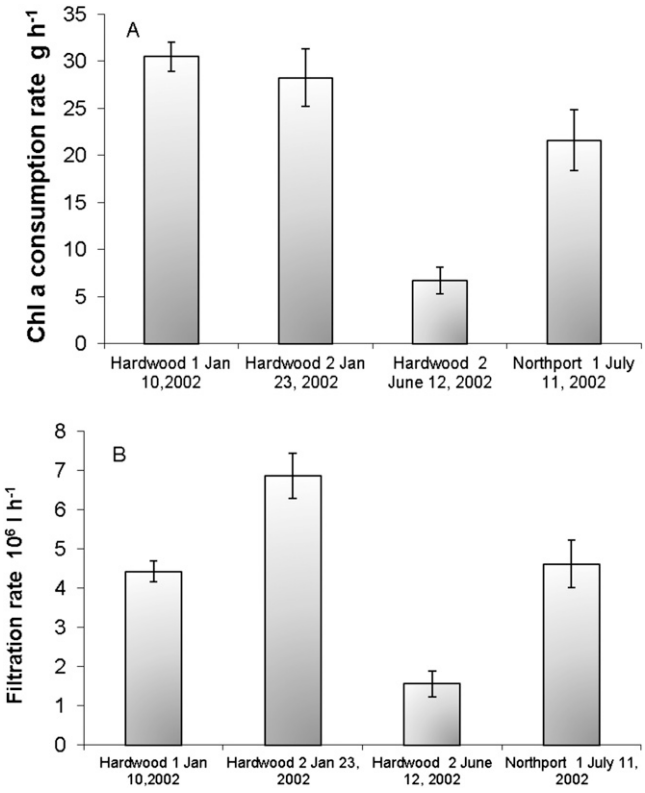

Figure 12. (A, B) Chlorophyll *a* (chl *a*) consumption rate (A) and filtration rate (B) of individual mussel rafts based on long-term (2–4 days) measurements of chl *a* inside and outside the rafts, and flow speed in the rafts. Values are mean ± SE.

$$300\,\text{ropes: } V = 0.4x^2 - 3.3x + 10.5 \tag{19}$$

$$400\,\text{ropes: } V = 0.35\,x^2 - 3.05\,x + 9.7 \tag{20}$$

$$500\,\text{ropes: } V = 0.35\,x^2 - 30.5\,x + 9 \tag{21}$$

DISCUSSION

The production capacity of a mussel raft is a function of the raft geometry, mussel biomass, water velocity, and food concentration (Cabanas et al. 1979, Heasman et al. 1998, Camacho et al. 1991, Petersen et al. 2008, the current study). Other factors important to growth are water temperature, food quality, and upstream mussel density. Raft geometry affects the productive capacity by controlling the VF passing through the raft, which is a function of the raft's cross-sectional area and

TABLE 6.

Probability values of the effects of outside chl *a* or inside current speed on the chl *a* consumption rate or clearance rate of mussels in the rafts for the long-term (2–4 days) experiments.

Period	Effect	Chl *a* consumption rate (μg/h)	Clearance rate (L/h)	*n**	Mean outside chl *a* (μg/L)	Mean current speed (cm/sec)
January 10–13	Current speed	0.0004†	0.20 NS	72	8.7	1.75
	Outside chl *a*	0.0008†	0.69 NS			
January 25–28	Current speed	0.64 NS	0.47 NS	68	7.41	2.15
	Outside chl *a*	0.006†	0.0001†			
June 12–13	Current speed	0.0001†	0.0002†	18	3.86	2.63
	Outside chl *a*	0.005†	0.01†			
July 11–13	Current speed	0.06† NS	0.0001†	31	5.48	4.41
	Outside chl *a*	0.0001	0.04			

* Hourly mean values. † Significant. NS, not significant.

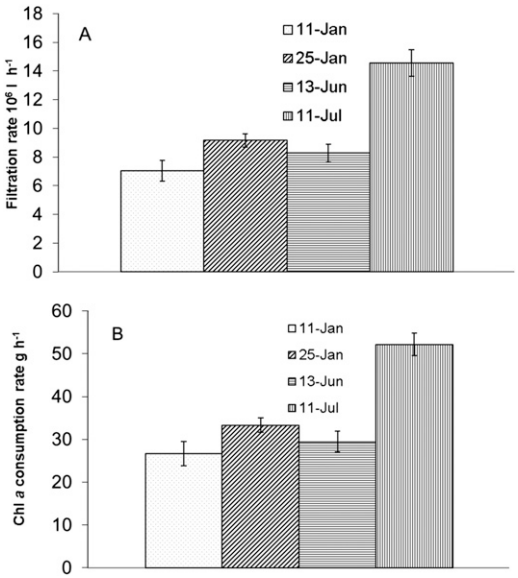

Figure 13. (A, B) Mean (± SE) filtration rate (A) and chlorophyll *a* consumption rate (B) for Maine mussel rafts at Hardwood Island and Northport, Maine, during periods when tidal flow direction had the outside CTD upstream from the rafts.

the frictional drag of the structure. The mussel raft size, orientation to flow direction, rope spacing, rope diameter, and predator nets all affect the VF through mussel rafts (Duarte et al. 2008, Delaux et al. 2011, Plew et al. 2011a, the current study). Grant et al. (1998) suggested that raft-scale water exchange, which is a function of the drag coefficient of the mussel ropes (see also Duarte et al. (2008)), limits the secondary production of mussel rafts. Because drag is proportional to the square of the velocity, the current reduction within the raft resulting from drag should result in raft velocity being the square root of the ambient velocity (Grant et al. (1998), and similar results in the current study). Rosland et al. (2011) also found that the spacing between ropes in longline systems affects mussel farm productivity. Grant and Bacher (2001) estimated that the longlines used for scallop and kelp culture in Sungo Bay, China, reduced the exchange rate of the culture sites by 41% as a result of the drag induced by the lantern net system. Plew (2011a) determined that longline shellfish farms may also reduce velocities within an embayment as a result of the drag of the mussel ropes within the "farm canopy" extending down from the surface. Furthermore, mussel farm drag was shown to increase seston depletion (as indicated by an increase in tracer concentrations in simulations with and without mussel farm drag) in inner bay regions where water residence time was increased (Plew 2011b). The same effects occur within mussel raft structures themselves (Fig. 9).

Particle consumption rates by mussels in rafts in Maine can be modeled by combining flow results with knowledge of mussel feeding rates. Consumption models using FLOW-3D, which combine mussel particle consumption with ambient hydrodynamics at the scale of the culture unit (i.e., a mussel raft), provide a novel 3-dimensional application of shellfish aquaculture modeling. The depletion model can also account for multiple rafts at various orientations, and mussel particle consumption rates can be specified (i.e., reducing at high flow rates or at low particle concentration levels).

When tide directions were known, mussel raft filtration rates and consumption rates of chl *a* increased with increasing food concentration outside the rafts (Table 7). Duarte et al. (2008) developed an analytical model to examine the carrying capacity of Galician mussel rafts as a function of water velocity and mussel stocking density, and demonstrated the importance of the drag of mussel ropes on mussel raft production as a function of seeding density. Duarte et al. (2008) used a constant clearance rate of mussels, although other workers (Winter 1976, Hawkins et al. 1996, Newell et al. 1998, Newell et al. 2001, Riisgård et al. 2003) have shown that mussel clearance rates may vary according to food availability, and Newell et al. (2001) demonstrated that responses occur over short timescales.

Mussel raft consumption of chl *a* increased with current velocity over a range of 1–8 cm/sec. At the Northport site, which had twice the VF through the mussel rafts as the Hardwood Island, 50 g chl *a*/h (and 15 million L/h filtered) were consumed by mussels in the raft in contrast to 30 g/h at Hardwood Island (and 8 million L/h filtered). Measured rates of POC consumption (100–400 g/h) at the Maine sites were considerably less than the POC consumption of 2,866 g/h/raft for mussels in a Spanish raft, which is 4 times the surface area (Cabanas et al. 1979), and where reported current speeds and POC concentrations are greater than in Maine.

A comparison between our data on mussel raft VF, filtration rates, and consumption of chl *a* with those from Cabanas et al.

TABLE 7.

Probability values of the effects of outside chl *a* or inside current speed on mussel raft consumption rate or clearance rate for segments of the long-term experiments only when tidal direction was constant.

Period	Effect	Chl *a* consumption rate (μg/h)	Clearance rate (L/h)	*n*	Time (h)	Mean outside chl *a* (μg/L)	Mean current speed (cm/sec)
January 11	Current speed	0.011*	0.0352	59	10	6.35	1.49
	Outside chl *a*	0.0000*	0.0000*				
January 25	Current speed	0.3827 NS	0.677 NS	240	4	6.25	1.43
	Outside chl *a*	0.0000*	0.0012*				
June 13	Current speed	0.0004	0.0003*	162	2.5	4.01	4.33
	Outside chl *a*	0.0000*	0.0000*				
July 12	Current speed	0.0008*	0.34 NS	140	4.5	4.36	6.68
	Outside chl *a*	0.0000*	0.0238*				

* Significant. NS, not significant.

TABLE 8.

Mussel density and biomass samples from mussel rafts at Hardwood Island and Northport, ME, from 1999 to 2003.

Date	Location	Density (mussels/m)	Biomass (g/m)	Total biomass (kg/raft)
August 1, 1999	Hardwood	976 (292)	522 (127)	2,297 (559)
December 5, 1999	Hardwood	896 (205)	903 (80)	3,977 (353)
August 21, 2002	Hardwood	552 (166)	617 (200)	2,715 (882)
January 8, 2003	Hardwood	1,064 (115)	1,390 (330)	6,116 (1,454)
March 19, 2003	Northport	1,063 (89)	1,137 (48)	5,004 (213)

Values are mean (±standard error).

(1979), Boyd and Heasman (1998), and Heasman et al. (1998) are presented in Table 9. Because of the greater rope density ($2.8/m^2$) and longer ropes on Maine mussel rafts, filtration rate per square meter of culture area was greater in Maine than at the sites in Spain and South Africa with lower rope densities ($1.5–2/m^2$).

Using observed filtration rates in the feeding chambers, we may estimate the demand of a mussel raft based on its biomass. For values of 3,941 kg/raft and 7,240 kg/raft, mussel filtration rates would be 12.6×10^6 L/h and 23.1×10^6 L/h, respectively, for the mean and maximum raft biomass observed on the Maine mussel rafts. These values were observed as maximum filtration rates at both Hardwood Island and Northport, but mean daily values were about one-third those values.

At sites with high tidal currents, direct inhibition of mussel feeding resulting from high velocities would be expected on the corners of the raft. At high water velocities on the edges of the rafts, but with adequate food levels, mussels may keep their valves open and close the inhalant siphon partially to allow for some particle uptake, although at reduced uptake levels relative to lower current velocities (Newell et al. 2001). The effects of inhibitory water velocities are a function of mussel orientation to flow direction and will vary within the position on a mussel rope. Computational fluid dynamics analysis has demonstrated that most of the raft area is characterized by low velocities, which are only 20%–25% of the flow outside the rafts. When the 25% reduction in flow velocity resulting from predator nets is also included in the calculations, ambient flow velocities of 11–44 cm/sec outside the rafts will result in optimum flow velocities for feeding (2–8 cm/sec) inside the mussel rafts.

When mussel biomass in a raft is high and water velocities are low, the consumption of food by the mussels results in chl *a* depletion in the middle of the raft. To minimize depletion and achieve a VF through the rafts that exceeds the raft's filtration capacity (i.e., $10–20 \times 10^6$ L/h), recommended flow speeds through Maine mussel rafts with a cross-sectional area of 121 m^2 requires a minimum outside flow speed of 14–23 cm/sec.

The presence of waves at some exposed sites may result in differences in water velocity with depth. Current profiling using the ADP in Northport demonstrated that depth-averaged velocities underestimated surface (depth, 0–2 m) current velocities, which exceeded 80 cm/sec in some instances during windy periods. Along the vertical culture ropes, mussels near the top may experience greater velocities, whereas the mussels 3–10 m deeper may benefit from a gentler environment. Because the orbital velocities of waves decrease rapidly with depth, it is likely that at exposed sites, near-surface waters may reach velocities that inhibit feeding, whereas deeper locations may be exposed to the "optimal velocity" for longer periods of time. Prolonged exposure to wave action or high tidal currents results

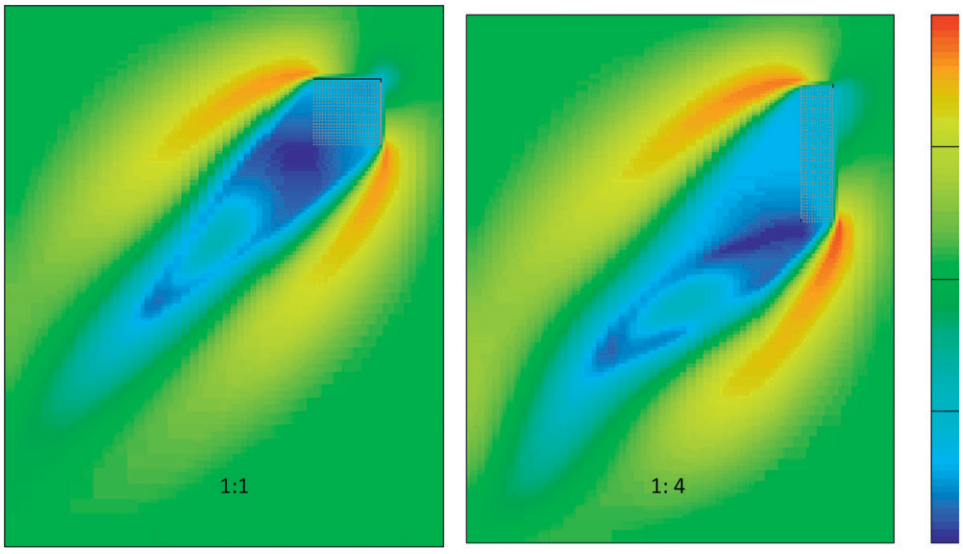

Figure 14. Effects of mussel raft aspect ratio on mean water velocity (plan view) for test conditions from the Hardwood Island, Maine, site with a 45-deg orientation of flow direction. Units are centimeters per second.

TABLE 9.

Mussel raft volume flux, clearance rate, chlorophyll consumption, and filtration rate per square meter of mussel raft surface area from published values and this study.

Location	Volume flux (L/h × 10^6)	Clearance rate (L/h × 10^6)	Consumption rate of chl *a* (g/h)	Raft surface area (m^2)	Cr (L/h m^{-2})
Spain*	31.7	14.9	11.9	528	28,220
Hardwood, ME	7.1	8	30	144	55,556
Northport, ME	31.8	14.5	52	144	100,694
South Africa†	3.8	6.1	14.6	242	25,207

* Values from Spain are from mean values over a 20-day period (Cabanas et al. 1979).
† Values from South Africa use mean current velocities (Boyd & Heasman 1998) and chl *a* consumption from Heasman et al. (1998, Table 1).

in slower growth rates of mussels (Harger 1970) and changes in shell shape (Seed 1968). At exposed locations, the development of a submersible raft may have benefits for increased feeding and growth rates of cultivated mussels.

CONCLUSIONS

The effects of hydrodynamics on the food supply and demand of mussel rafts have been characterized using a combination of field data collection and computer modeling using FLOW-3D. FLOW-3D is a useful tool to model complex, culture unit-specific particle flux and consumption rates, and to provide insight into sampling strategies that allow for the characterization of the production efficiency of shellfish aquaculture structures such as mussel rafts, longlines, oyster rack and bags, and floating oyster trays. Values estimated using the model and field data indicate that mussel raft hydrodynamics are a function of raft orientation to current direction, mussel raft size, raft aspect ratio, the presence of predator nets, the presence of multiple rafts, rope spacing, and rope diameter. Flow through mussel rafts is not very sensitive, however, to the water depth under the rafts. For even distribution of food throughout mussel rafts, they should be moored on both sides and placed in locations where current direction alternates between flood and ebb tides. Rafts moored on 1 side only, or in locations where flow is unidirectional, may result in poor food availability on the downstream side of the rafts.

Mussel raft consumption can be estimated efficiently by two methods: (1) profiles of chl *a* and current speed with depth upstream and inside the rafts, and (2) long-term measurements of chl *a* and current speed in the middle of a raft at mid depth and chl *a* at a control station outside the raft also at mid depth.

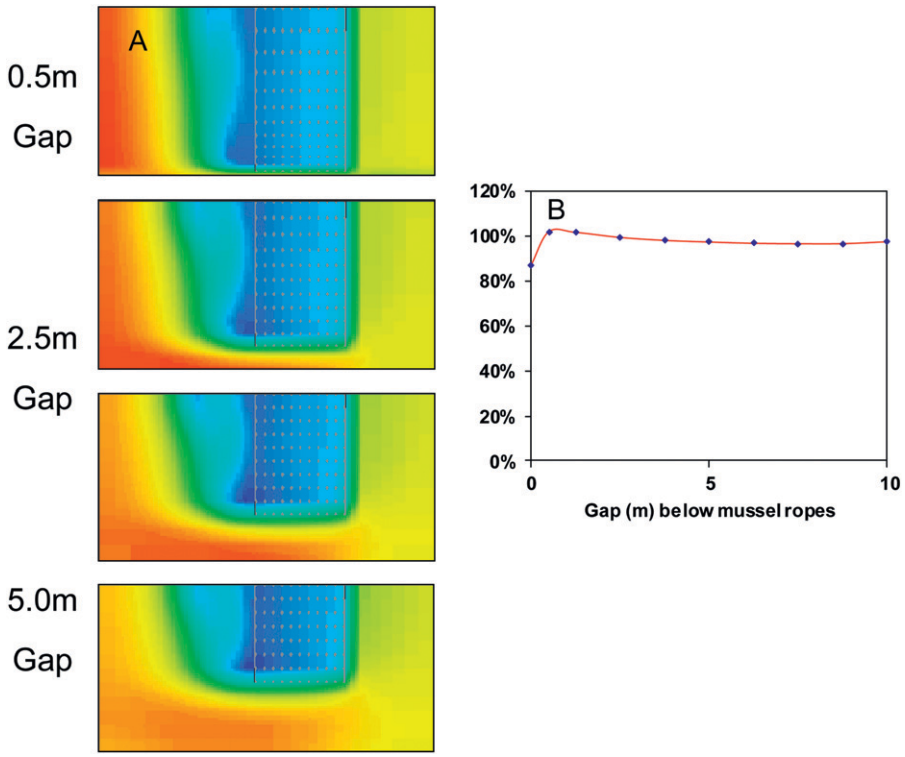

Figure 15. Velocity at bottom of mussel ropes as a percent of the average velocity through the entire mussel raft. (A) Vertical section of mussel raft (colored by velocity) with gaps of 0.5, 2.5, 5.0, and 7.5 m between the mussel ropes and the seabed. (B) Graph of percent velocity versus gap distance.

Field measurements demonstrate a significant positive effect of food concentration on the clearance rates and consumption rates of chl *a*, and organic carbon and nitrogen by mussels in floating rafts, and a positive effect of water velocity on the consumption rates of chl *a*. The production capacity of mussel rafts is ultimately limited by the supply of ambient phytoplankton, which increases with increased water velocity through the rafts. Measurements of clearance rates by mussels in rafts indicate a minimum ambient velocity of 10 cm/sec below which it is expected that growth will be limited by food flux. In contrast, the clearance rates of individual mussels are limited by flows greater than 10 cm/sec. The production capacity of rafts at sites with lower currents may be increased by adjusting raft size, geometry, orientation to flow direction, and stocking density (Eqs (16)–(21)).

In addition to estimating the effects of different husbandry strategies on mussel raft hydrodynamics, FLOW-3D was used to determine optimal locations for sampling sites to estimate water VF and the consumption of particles by mussels in an entire raft. Measurements of water velocity taken in the middle of the raft at mid depth underestimate flow through the raft by 10%, and measurements of water velocity and chl *a* concentration taken at the middle of the raft at mid depth underestimate particle consumption rates by 13%. These adjustment factors can be applied to field measurements to estimate integrated and mean culture unit (raft) scale hydrodynamics and particle consumption characteristics.

In summary, the effects of raft culture systems on flow through the rafts is presented. Our study shows the following:

1. Rectangular (or square) rafts should be oriented 45 deg to the flow to maximize the mean flow speed through the rafts. Any change in orientation other than parallel to flow direction will improve the flow through the raft structure, resulting from an increase in raft cross-sectional area.
2. The aspect ratio of rectangular rafts should be as large as possible to maximize the mean flow speed through the rafts. This may also be accomplished using multiple raft systems
3. Nonuniform spacing (e.g., gaps) between droppers can be used to increase the average flow speed through rafts.
4. In multiple raft operations, the position of adjacent rafts can be chosen to maximize the average flow speed through the raft array.
5. The number of ropes and their spacing play a critical role in controlling the circulation of water through the floating raft structures, and should be chosen such that the flow of water through the rafts is not choked during the final phases of the grow-out cycle. By removing 3 parallel strips of ropes in the raft, water velocity can be increased by 20%.
6. The circulation of the waters beneath the raft structures is not very sensitive to rope length (Fig. 15).
7. The mean water velocity through the rafts as a percentage of the external velocity remains constant for a given raft configuration.
8. The circulation of waters through the raft structures is sensitive to raft size. Rafts should, therefore, be sized according to local flow conditions (e.g., smaller rafts should be used at sites where ambient flow velocities are low).

ACKNOWLEDGMENTS

This material is based on work supported by the Cooperative State Research, Education and Extension Service, U.S. Department of Agriculture, under SBIR agreement no. 2001-03298 to Great Eastern Mussel Farms, Inc. We acknowledge Alden Laboratories, Jessie Munro, Charles Gregory, Shawn Robinson, Charlie Yentsch, Bruce MacDonald, Anne Langston, and anonymous reviewers for helpful comments.

LITERATURE CITED

Bayne, B. L., J. Iglesias, A. Hawkins, E. Navarro, M. Heral & J. M. Deslous-Pali. 1993. Feeding behavior of the mussel *Mytilus edulis*: responses to variations in quantity and organic content of the seston. *J. Mar. Biol. Assoc. UK* 73:813–829.

Blanco, J., M. Zapata, & A. Morono. 1996. Some aspects of the water flow through mussel rafts. *Sci. Mar*. 60:275–282.

Boyd, A. J. & K. G. Heasman. 1998. Shellfish mariculture in the Beneguela system: water flow patterns within a mussel farm in Saldanha Bay, South Africa. *J. Shellfish Res*. 17:25–32.

Cabanas, J. M., J. J. Gonzalez, J. Marino, A. Perez & G. Roman. 1979. Estudio del mejillon y de su epifaunal en los cultivol flotantes de la Ria de Arosa: III. Observaciones previas sobre la retencion de particulas y la biodeposicion de una batea. *Bol. Inst. Esp. Oceanogr*. 5:43–50.

Camacho, A. P., R. Gonzalez & J. Fuentes. 1991. Mussel culture in Galicia (N.W. Spain). *Aquaculture* 94:263–278.

Coughlan, J. 1969. The estimation of filtration rate from the clearance of suspensions. *Mar. Biol*. 2:356–358.

Cubillo, A. M., L. G. Peteiro, M. J. Fernández-Reiriz & U. Labarta. 2012. Density-dependent effects on morphological plasticity of *Mytilus galloprovincialis* in suspended culture. *Aquaculture* 338:246–252.

Delaux, S., C. L. Stevens & S. Popinet. 2011. High-resolution computational fluid dynamics modelling of suspended shellfish structures. *Environ. Fluid Mech*. 11:405–425.

Duarte, P., U. Labarta & M. J. Fernández-Reiriz. 2008. Modelling local food depletion effects in mussel rafts of Galician Rias. *Aquaculture* 274:300–312.

Fréchette, M., M. Lachance-Bernard & G. Daigle. 2010. Body size, population density and factors regulating suspension-cultured blue mussel (*Mytilus* spp.) populations. *Aquat. Living Resour*. 23:247–254.

Fuentes, J., V. Gregorio, R. Giraldez & J. Morales. 2000. Within-raft variability of the growth rate of mussels, *Mytilus galloprovincialis*, cultivated in the Ria do Arousa NW Spain. *Aquaculture* 189:39–52.

Gibbs, M. M., M. R. James, S. E. Pickmere, P. H. Woods, B. S. Shakespeare, R. W. Hickman & J. Illingworth. 1991. Hydrodynamic and water column properties at six stations associated mussel farming in Pelorus Sound, 1984–1985. *N. Z. J. Mar. Freshw. Res*. 25:239–254.

Grant, J. & C. Bacher. 2001. A numerical model of flow modification induced by suspended aquaculture in a Chinese Bay. *Can. J. Fish. Aquat. Sci*. 58:1003–1011.

Grant, J., J. Stenton-Dozey, P. Monteiro, G. Pitcher & K. Heasman. 1998. Shellfish mariculture in the Beneguela system: a carbon budget of Saldanha Bay for raft culture of *Mytilus galloprovincialis*. *J. Shellfish Res*. 17:41–49.

Harger, J. R. E. 1970. The effect of wave impact on some aspects of the biology of sea mussels. *Veliger* 12:401–414.

Hawkins, A. J. S., R. F. M. Smith, B. L. Bayne & M. Heral. 1996. Novel observations underlying the fast growth of suspension-feeding shellfish in turbid environments: *Mytilus edulis*. *Mar. Ecol. Prog. Ser*. 131:179–190.

Heasman, K. G., G. C. Pitcher, C. D. McQuaid & T. Hecht. 1998. Shellfish mariculture in the Beneguela system: raft culture of *Mytilus galloprovincialis* and the effect of rope spacing on food extraction, growth rate, production and condition of mussels. *J. Shellfish Res*. 17:33–39.

Hirt, C. W. 2010. FLOW-3D users manual. Santa Fe, NM: Flow Science, Inc.

Iglesias, J. I. P., E. Navarro, P. Alvarez-Jorna & I. Armetia. 1992. Feeding, particle selection and absorption in cockles *Cerastoderma edule* (L.) exposed to variable conditions of food concentration and quality. *J. Exp. Mar. Biol. Ecol*. 162:177–198.

Newell, C. R. 1990. A guide to mussel quality control. Maine Sea Grant Technical Report E-MSG-90-1. 17 pp.

Newell, C. R., D. E. Campbell & S. M. Gallagher. 1998. Development of the mussel aquaculture lease site model MUSMOD: a field program to calibrate model formulations. *J. Exp. Mar. Biol. Ecol.* 219:143–169.

Newell, C. R., D. J. Wildish & B. A. MacDonald. 2001. The effects of velocity and seston concentration on the exhalant siphon area, valve gape and filtration rate of the mussel *Mytilus edulis*. *J. Exp. Mar. Biol. Ecol*. 262:91–111.

Petersen, J. K., T. G. Nielsen, L. A. Duren & M. Maar. 2008. Depletion of plankton in a raft culture of *Mytilus galloprovincialis* in Ría de Vigo, NW Spain: I. Phytoplankton. *Aquat. Biol*. 4:113–125.

Plew, D. R., M. P. Enright, R. I. Nokes & J. K. Dumas. 2009. Effect of mussel bio-pumping on the drag on and flow around a mussel crop rope. *Aquacultural Engineering,* 40:55–61.

Plew, D. R. 2011a. Depth-averaged drag coefficient for modeling flow through suspended canopies. *J. Hydraul. Eng*. 137:234–247.

Plew, D. R. 2011b. Shellfish farm-induced changes to tidal circulation in an embayment, and implications for seston depletion. *Aquacult. Environ. Interact*. 1:201–214.

Riisgård, H. U., C. Kittner & D. F. Seerup. 2003. Regulation of opening state and filtration rate in filter-feeding bivalves (*Cardium edule, Mytilus edulis, Mya arenaria*) in response to low algal concentration. *J. Exp. Mar. Biol. Ecol*. 284:105–127.

Rosland, R., C. Bacher, O. Strand, J. Aure & T. Strohmeier. 2011. Modelling growth variability in longline mussel farms as a function of stocking density and farm design. *J. Sea Res*. 66:318–330.

Seed, R. 1968. Factors influencing shell shape in the mussel *Mytilus edulis*. *J. Mar. Biol. Assoc UK* 48:561–584.

Strathmann, R. R. 1967. Estimating the organic carbon content of phytoplankton from cell volume or plasma volume. *Limnol. Oceanogr*. 12:411–418.

Winter, J. E. 1976. A critical review on some aspects of filter-feeding in lamellibranchiate bivalves. *Haliotis* 7:71–87.

Yentsch, C. S. & D. W. Menzel. 1963. A method for the determination of phytoplankton chlorophyll and phaeophytin by fluorescence. *Deep-Sea Res*. 10:221–231.